# RIG-I acts as a tumor suppressor in melanoma via regulating the activation of MKK/p38MAPK signaling pathway

**Rui Guo**
Shanghai Jiao Tong University Medical School Affiliated Ruijin Hospital
**Shun-Yuan Lu**
Shanghai Jiao Tong University Medical School Affiliated Ruijin Hospital
**Jin-Xia Ma**
Shanghai Jiao Tong University Medical School Affiliated Ruijin Hospital
**Qian-Lan Wang**
Shanghai Jiao Tong University Medical School Affiliated Ruijin Hospital
**Lu Zhang**
Shanghai Jiao Tong University Medical School Affiliated Ruijin Hospital
**Ling-Yun Tang**
Shanghai Jiao Tong University Medical School Affiliated Ruijin Hospital
**Yan Shen**
Shanghai Jiao Tong University Medical School Affiliated Ruijin Hospital
**Chun-Ling Shen**
Shanghai Jiao Tong University Medical School Affiliated Ruijin Hospital
**Jin-Jin Wang**
Shanghai model organisms center
**Li-Ming Lu**
Shanghai Institute of Immunology
**Zhu-Gang Wang**
Shanghai Jiao Tong University Medical School Affiliated Ruijin Hospital
**Hong-Xin Zhang** (✉ zhang_hongxin@hotmail.com)
Shanghai Jiao Tong University Medical School Affiliated Ruijin Hospital https://orcid.org/0000-0002-3649-2065

---

**Research article**

**Keywords:** Retinoic acid-inducible gene I, Melanoma, Proliferation, Apoptosis, p38 MAPK

**Posted Date:** July 30th, 2021

**DOI:** https://doi.org/10.21203/rs.3.rs-758070/v1



**Version of Record:** A version of this preprint was published at Human Cell on April 13th, 2022. See the published version at https://doi.org/10.1007/s13577-022-00698-1.

## Abstract

# Background

Studies have indicated that RIG-I may act as a tumor suppressor and participate in the tumorigenesis of some malignant diseases. However, RIG-I induces distinct cellular responses via different downstream signaling pathways depending on the cell type. The aim of this study was to investigate the biological function and underlying molecular mechanism of RIG-I in the tumorigenesis of melanoma.

# Methods

We conducted *RIG-I* knockout and RIG-I overexpressing B16-F10 melanoma cell line, and further analyzed the RIG-I mediated change of tumor biology behaviors in spontaneous and poly I:C induced RIG-I activation status. Cell proliferation, cell cycle, apoptosis and migration were detected by CCK-8 assay, BrdU incorporation, Annexin V-PI staining assay and transwell assay, respectively. In vivo tumorigenicity was evaluated by tumor xenograft growth in nude mice and subsequently Ki67 staining and TUNEL assay. Furthermore, Western blot was utilized to explore the underlying mechanism of RIG-I in melanoma cells.

# Results

Our data showed that RIG-I promotes the apoptosis and inhibits the proliferation by G1 phase cell-cycle arrest in B16-F10 melanoma cell line. Mechanically, RIG-I could induce the phosphorylation level of p38 MAPK and MAPK kinase MKK3/MKK4.

# Conclusion

The current study demonstrated that RIG-I suppressed the development of melanoma via regulating the activity of MKK/p38 MAPK signaling pathway, which will be useful in the research of novel therapeutic targets for this malignant disease.

## Introduction

Melanoma is one of the most malignant and aggressive type of skin cancer, accounting for more than 80% of skin cancer-associated deaths in the world [1]. In the past several decades, the annual incidence and range of onset areas of melanoma have increased rapidly [2]. Although many therapeutic methods including surgical resection, combined chemotherapy, photodynamic therapy, radiotherapy and molecular targeted therapy, have been extensively used for the treatment of melanoma, the overall 5-year survival rate for patients remains poor [3, 4]. Therefore, it is urgent to investigate melanoma biology and to identify novel risk factors involved in the development of melanoma, which will be helpful to find

effective methods for the prevention, diagnosis and early therapeutic strategies of this disease. At present, a number of factors have been demonstrated to be associated with the development of melanoma, including phenotypic, genetic and environmental risk factors [5, 6]. In the last several decades, a number of genes related to the pathogenesis of melanoma have been identified by genetic studies [7–9].

Retinoic acid-inducible gene I (RIG-I), also known as DDX58, is the charter member of the RLR (RIG-I -like receptors) family, which are important cytosolic virus recognition molecule in the innate antiviral immune responses [10]. RIG-I is a kind of DExD/H box-containing RNA helicase and consists of two amino (N) -terminal caspase activation and recruitment domains (CARD) in tandem, a central DExH/C box ATPase domain and a carboxy-terminal regulatory/repressor domain (RD) [11]. In the absence of ligand RNA, RIG-I adopts an auto-inhibitory conformation. After binding to appropriate RNA, it undergoes conformational changes that exposes the CARDs and then binds and activates the adaptor protein MAVS (mitochondrial antiviral signaling protein) via homotypic CARD-CARD interaction [12–14]. MAVS subsequently acts as a scaffold by recruitment and activation of downstream signaling molecules, including TBK1/IKK-i and IKKα/IKKβ complexes, which further facilitates activation of transcriptional factors IRF3/IRF7 and NF-κB, respectively. Activated IRF3 and NF-κB then induce the expression of type I interferons and some other related genes that eventually provide an antiviral state for host cells [10, 15]. Intriguingly, accumulating evidence indicates that RIG-I is also involved in a series of cellular and physiological processes such as inflammation and inflammatory diseases, cell proliferation, apoptosis, senescence and even carcinogenesis [16, 17]. Our previous work have reported that RIG-I deficient mice developed a colitis-like phenotype and prone to colitis-associated colorectal cancer [18, 19]. Some other studies also indicate that may function as a tumor suppressor, and seems that RIG-I may involve different signaling pathways in a cell specificity manner [20, 21].

Several studies have revealed that RIG-I participates in the progression of interferon-α-induced apoptosis in tumor-repopulating cells of melanoma [22], and involves in the apoptosis of melanoma cells in response to its agonist poly I:C [23]. However, the precise roles of RIG-I in the pathogenesis and treatment have not yet been fully elucidated. To further clarify the biology function of RIG-I in the pathology of melanoma, we analyzed the effects of RIG-I on the tumor biological behaviors with or without poly I:C using *RIG-I*-knockout (KO) and RIG-I-overexpressing B16-F10 melanoma cell line. Our data indicated that RIG-I participate in the proliferation and apoptosis via MKK4-p38 MAPK signaling cascade. These findings uncovered an important novel role of RIG-I in the tumorigenesis of melanoma.

## Materials And Methods

## Cell culture and poly I:C treatment

B16-F10 murine melanoma cells were obtained from the Cell Bank of Shanghai Institute of Cell Biology (Shanghai, China). Cells were maintained high-glucose Dulbecco's Modified Eagle Medium (DMEM) (Hyclone, USA), supplemented with 10% fetal bovine serum (FBS, Gibco, USA) .Cells were cultured at 37°C

in a humidified 5% $CO_2$ atmosphere. Once RIG-I knockout and RIG-I overexpression B16-F10 cells reached 80% confluence in cell culture plate, the cells were cultured in fresh complete DMEM and transfected with poly I:C (10μg/ml) for 24h using Lipofectamine 3000 Transfection Reagent (Invitrogen, USA), according to the manufacturer's instructions.

**Knockout and overexpression of RIG-I.**

*RIG-I*-knockout B16-F10 melanoma cell line was generated using the CRISPR-Cas9 gene editing system. Briefly, the guide-RNA for RIG-I was designed by the online CRISPR design tool (https://zlab.bio/guide-design-resources), the two complementary oligonucleotides were shown as follow: sgRNA-1: 5'-CTACATGAGTTCCTGGCTCG-3' and sgRNA-2: 5'-AAACCGAGCCAGGAACTCATGTAGC-3'. Cas9 sgRNA vector was digested with BbsI and gel purified. The oligonucleotides were annealed and cloned into the BbsI-digested Cas9 PX459 vector. The empty vector was used as the control, 4μg plasmids were transfected into B16-F10 cells using Lipofectamine 3000 Transfection Reagent (Invitrogen, USA). After 48h, the cells were incubated in DMEM with 4μg/mL puromycin for 7 days. Cells resistant to puromycin could be selected, and Western blot analysis was used to identify the effect of knockout. The expressing vector of RIG-I were described previously [24], briefly, full length RIG-I cDNA were amplified by PCR using the primers with Kpn I or Not I site (5'-ACTGGTACCATGACCGCGGCGCAGCGGCA-3' and 5'-ACTGCGGCCGCTCATACGGACATTTCTGCAG-3'). The PCR products were digested with Kpn I and Not I, and cloned into the corresponding sites in pCMV-Myc vector. The vector was confirmed by sequencing and further transfected into B16-F10 cells.

# Western Blotting

Cells were collected and lysed using RIPA buffer (Beyotime, China) with fresh protease inhibitor cocktail and phosphatase inhibitor (Roche, Switzerland), the cell lysates were collected and centrifuged at 12,000 rpm and 4°C for 10 min. The supernatants were collected carefully and the concentration was quantified by BCA Protein Assay Kit (Thermo Fisher, USA). Each sample contained an equal concentration of 30 μg of proteins. The samples were heated at 100°C for 5 min, and 20 μL of each sample was loaded onto an 8% sodium dodecyl sulfate (SDS)-polyacrylamide gel and electrophoresed. Isolated proteins were transferred onto a nitrocellulose filter (NC) membrane then blocked with 5% non-fate skim milk in PBS and shaking for 1h.The membranes were incubated with primary antibodies against RIG-I (1:1000, D14G6, Cell Signaling, USA), P-MKK3 (1:1000, 12280, Cell Signaling, USA), MKK3(1:1000, 8535, Cell Signaling, USA), P-MKK4 (1:1000, 4514, Cell Signaling, USA), MKK4 (1:1000, 9152, Cell Signaling, USA), P-p38(1:1000, 9211, Cell Signaling, USA), p38 (1:1000, 9212, Cell Signaling, USA), Cyclin D1(1:1000, 9932, Cell Signaling, USA), and GAPDH (1:2000, D110016, BBI, China) overnight at 4°C. Then the membranes were washed three times with PBST for 5 min and incubated with IRDyeCW800-conjugated anti-rabbit immunoglobulin (LI-COR) for 1h at room temperature and scanned with the LI-COR Odyssey imaging system (LI-COR).

# CCK8 Cell Viability Assay

B16-F10 murine melanoma cells were seeded into the 96-well plates (7500/per well). After the cells were attached (0 h), 10 μL of CCK8 (Dojindo, Japan) was added to the culture plate, which was incubated for 1h at 37°C in a humidifier. The absorbance at 450 nm of each well was recorded by a microplate reader (BioTek, USA). Cells were subjected to transfected with or without 10μg/ml poly I:C at 37°C for 24 h and the absorbance value was measured.

# BrdU incorporation and apoptosis detection

B16-F10 murine melanoma cells were plated into 6-well plates ($2 \times 10^5$/per well) and cultured for 24h, cells were treated with or without poly I:C for 24h. For apoptosis assays, cells were harvested and marked with APC-Annexin V and PI using Annexin V APC Apoptosis Detection Kit (eBioscience, USA) and according to the manufacturer's instructions. For proliferation assays, cells were loaded with BrdU (5μg/ml) for 1h and stained with anti-BrdU then marked with 7-AAD using BrdU Cell Proliferation Kit (Biolegend, USA). The results were evaluated with FlowJo software.

**Cell migration assay.**

Migration assay was performed using Millipore Transwell system chambers (8-μm pore size, Millipore, USA). $5 \times 10^4$ cells were seeded into the upper chambers of 24-well plates in 400 μl serum-free DMEM while the lower chambers were filled with 600 μl complete medium with 3μg/ml Mitomycin. The plate was incubated at 37°C for 48h.Then the cells in upper chambers were removed with cotton swab and the lower chambers were fixed with 4%PFA for 10 mins at room temperature and stained with 0.5% crystal violet in 10% methanol and photographed at ·200 magnification.

# In vivo experiments

Fourteen 6-week-old specific pathogen-free BALB/c female nude mice weighting 20-25g were purchased from Phenotek Biotechnology (Shanghai) Co.,Ltd and maintained in specific pathogen-free conditions, with each mouse in an independent ventilation cage, at 20–26°C and humidity 40–70%, on a 12/12-h light/dark cycle (lights on at 06:00 h). Mat and feed were changed every 3 days. For the tumor challenge, $5{\cdot}10^5$ *RIG-I* knockout B16-F10 melanoma cells or control B16-F10 melanoma cells in 50 μl of serum-free DMEM were injected subcutaneously into the right flank area of nude mice. The mice were randomly divided into two groups using a computer based random order generator. There were seven animals in each group. One group of mice were injected with control B16-F10 melanoma cells while the other group mice were injected with *RIG-I* knockout B16-F10. For the experimental group and the control group, a mouse was randomly selected and permanently marked with a number. Measurements of tumor growth were started when the tumors grew 2 to 3 mm in diameter and were visible. Tumors were observed daily and the size of tumor were measured each 3–4 days. The measurement time is from 2:00 p.m. to 4:00 p.m. and the measurement sequence is in accordance with the number of mice. The mice were sacrificed on day 20 after implantation. All mice were euthanized with CO2. The initial process of CO2 delivery to the micro-isolator is completed by opening the CO2 cylinder valve, so that the mice will slowly be exposed to increasing CO2 levels (displacement per minute is about 30% of the cavity volume). After the color of

the eyes disappeared and breathing stopped, the flow of carbon dioxide was maintained for 5 minutes to confirm death. Tumor tissues were prepared for immunostaining. All experimental manipulations were approved by the Animal Ethics Committee of Ruijin Hospital Affiliated to Shanghai Jiao Tong University School of Medicine. Our research was in compliance with the institutional guidelines for care and use of animals.

# Immunofluorescence

The tumor tissue samples were fixed with 4% paraformaldehyde at 4°C overnight, then embedded with paraffin, and cut into 3-um-thick sections. The sections were deparaffinized, rehydrated, subsequently subjected to antigen retrieval. The sections were blocked in blocking buffer (10 % goat serum in 0.5% Triton X-100) for 30 min, and then incubated with primary antibody of Ki67 (1:1000, ab15580, Abcam, USA) overnight at 4°C. Then the slices were washed with 0.5% Triton X-100 three times and incubated with Alexa Flour 594 chicken anti-rabbit IgG(H + L) (1:500, A21442, Invitrogen, USA) and DAPI (1:1000) for 2h at room temperature. Apoptotic cells in the tumor tissue sections were quantified using the in situ Cell Death Detection Kit (Roche, Switzerland). The sections were visualized by a fluorescent microscope (Nikon, Japan) using appropriate excitation and emission spectra at x400 magnification.

# Statistical analysis

Statistical analysis was performed with SPSS software (version 20.0, SPSS, USA). All data are shown as the mean ± SD. For the count of Ki67 positive cell and TUNEL positive cell in mice, Student's *t*-test was used. For tumor volume, CCK8 cell viability assay, BrdU assay and APC-Annexin V assay were estimated with two-way ANOVA. Statistical significance was defined as $P < 0.05$.

## Results

**Generation of** RIG-I**-KO cell lines with CRISPR-Cas9 gene editing system.**

The CRISPR-Cas9 gene editing system was used to generate a *RIG-I*-knockout melanoma cell line. The oligonucleotides for the guide RNA were designed, synthesized and cloned into the pX459 vector (Fig. 1A). Then, the vectors were transfected into B16-F10 cells. The indel mutations in these cell lines were confirmed by DNA sequencing of the PCR products of target DNA (Fig. 1B). Finally, Western blot with anti-RIG-I antibody showed that the expression of RIG-I protein was abolished in the *RIG-I*-KO cell line (Fig. 1C).

# RIG-I plays a suppressible role in the proliferation of melanoma cells

The effect of RIG-I deficiency on the growth of B16-F10 cells was first evaluated by CCK-8 assay. As shown in Fig. 2A, the relative cell viability of B16-F10 cells was significantly increased in the *RIG-I* knockout group compared with that in the control group, both in the spontaneous and poly I:C stimulated state. To further elucidate the effects of *RIG-I* knockout on the proliferation capacity of B16-F10 cells, we

conducted a BrdU incorporation assay and assessed the cell cycle distribution using flow cytometry analysis. The results showed that target deletion of RIG-I resulted in decreased percentage of cells in the G0/G1 phase (Spontaneous: 64.97 ± 0.15% vs. 68.17 ± 0.85%, $P < 0.001$; poly I:C stimulation: 68.6 ± 0.50% vs. 80.93 ± 0.32%, $P < 0.0001$) and increased percentage of cells in the S phase (Spontaneous: 29.23 ± 0.46% vs. 25.3 ± 1.05%, $P < 0.01$; poly I:C stimulation: 22.30 ± 1.22% vs. 9.72 ± 0.52%, $P < 0.0001$) (Fig. 2B, C). These data suggested that target deletion of RIG-I promotes melanoma cell proliferation.

To further explore the role of RIG-I in the proliferation of melanoma cells, cell viability and cell cycle distribution were accessed in B16-F10 cells after transfection with RIG-I expressing vector or control vector. CCK-8 results showed that ectopic forced expression of RIG-I led to dramatic suppression of cell viability compared with control cells (Fig. 3A). As shown in Fig. 3B and C, RIG-I overexpression significantly increased the percentage of cells in G0/G1 phase (85.13 ± 0.64% vs. 74.45 ± 0.85%, $P < 0.0001$), and decreased the percentage of cells in S phase (5.46 ± 1.58% vs. 10.36 ± 2.90%, $P < 0.05$) and G2/M phase (6.42 ± 1.30% vs. 10.83 ± 3.07%, $P < 0.01$) in B16-F10 cells. These data indicated that RIG-I is able to suppress the proliferation of melanoma cells by arresting the cell-cycle in G1 phase.

# RIG-I plays a positive regulatory role in the apoptosis of melanoma cells

To clarify the effects of RIG-I on the apoptosis of melanoma cells, we performed Annexin V/PI staining assay and flow cytometry analyses. The results showed that the percentage of early apoptotic cells (Annexin $V^+/PI^-$, 0.28 ± 0.15% vs. 0.85 ± 0.17%, $P < 0.05$) were significantly decreased in *RIG-I*-KO cells compared with the control cells (Fig. 4A, B). We further observed that transfection of poly I:C could induce dramatic cell apoptosis. Both the poly I:C induced early (Annexin $V^+/PI^-$, 0.47 ± 0.18% vs. 1.51 ± 0.19%, $P < 0.01$) and late apoptosis (Annexin $V^+/PI^+$, 0.39 ± 0.05% vs. 0.80 ± 0.08%, $P < 0.01$) were significantly inhibited in *RIG-I* KO group. Then the effects of RIG-I overexpression on cell apoptosis was studied. The data revealed that both of the early (0.26 ± 0.06% vs. 0.10 ± 0.01%, $P < 0.05$) and late apoptosis (0.21 ± 0.04%vs. 0.06 ± 0.01%, $P < 0.05$) were dramatically increased in RIG-I overexpression melanoma cells compared with the control cells. As expected, ectopic forced expression of RIG-I significantly enhanced poly I:C induced apoptosis (Early apoptosis: from 2.37 ± 0.30% to 2.81 ± 0.17%, $P < 0.05$; Late apoptosis: from 1.61 ± 0.39% to 2.07 ± 0.56%, $P < 0.05$) (Fig. 4C, D). These results further confirmed the central role of RIG-I in the effects of poly I:C transfection on the melanoma cell line.

### RIG-I depletion does not affect the migration of melanoma cell.

To explore the role of RIG-I in the metastasis of melanoma, we assessed cell migration in vitro. Although the cell-matrix interaction was dramatically increased in the RIG-I-KO group, Transwell assay showed that the number of cells migrated out in the RIG-I-KO group was comparable with that in the control group (Figure S1). These data indicated that RIG-I is not the core factor in melanoma metastasis.

### Target deletion of RIG-I facilitates the growth of tumor xenografts in vivo.

After it was determined that RIG-I promoted the apoptosis and suppressed the proliferation of melanoma cells *in vitro*, the effects of RIG-I deletion on xenograft tumors in nude mice were investigated. As shown in Fig. 5A and B, The tumors in mice injected with *RIG-I*-KO cells showed obvious faster growth rate compared with the controls. The difference in tumor volume was significant after 20 days of subcutaneous injection ($P < 0.01$). The proliferative ability of the tumor xenografts was evaluated via histopathological staining for Ki67. The results showed that target deletion of RIG-I could induce the proliferation level in the tumor xenografts of B16-F10 cell (60.97 ± 13.56% vs. 35.96 ± 7.22%, $P < 0.001$) (Fig. 5C). Subsequently, apoptosis in the tumor tissue was examined using a TUNEL assay. The percentage of apoptotic cells in *RIG-I*-KO tumor xenografts (0.68 ± 0.32%) was significantly decreased compared with the control sample (1.61 ± 0.93%) (Fig. 5D). These results demonstrated that RIG-I deletion facilitated tumorigenesis in a xenograft tumor model *in vivo*.

**RIG-I regulates the growth of melanoma cell partially via MKK/p38 MAPK signaling cascade.**

To investigate the underlying mechanism through which RIG-I regulates the biological characteristics of melanoma cells, we analyzed the effects of RIG-I on the modulation of p38 MAPK pathways which have been demonstrated to be critical regulators in the proliferation and apoptosis of cancer cells. The results of western blotting showed that poly I:C induced phosphorylation of p38 MAPK signaling pathway-related proteins including p38 MAPK, MKK3 and MKK4 were notably decreased following knockout of *RIG-I*. Moreover, Cyclin D1, a downstream factor of p38 MAPK signaling pathway that promote cell cycle progression, was upregulated in *RIG-I*-KO cells (Fig. 6A, S2A). Conversely, ectopic overexpression of RIG-I upregulated the poly I:C induced phosphorylation of p38 MAPK, MKK3 and MKK4 (Fig. 6B, S2B). These results suggested that p38 MAPK signaling pathway may be involved in the effects of RIG-I on melanoma.

# Discussion

RIG-I is one of the most common cytosolic pattern recognition receptors, and its functions in the innate immune system have been well documented. However, accumulating evidence suggest that RIG-I is a multifunctional protein that functions far beyond being a pattern recognition receptor, and participates in various biological processes such as cell proliferation, apoptosis, aging, inflammatory diseases, detection of bacterial pathogens and even recognition of self mRNAs [16]. In the past several years, there is an increased interest in the potential role of RIG-I in the development and immune-therapy of many malignant diseases. Target activation of RIG-I by poly I:C or other agonists was previously tested as therapeutic strategy in some tumors [23, 25]. However, a line of studies have reported that RIG-I has distinct functions in malignant tumors according to their origins [20, 26, 27].

In the present study, the potential role of RIG-I in the biological characteristics of melanoma was assessed using a CRISPR-Cas9-mediated *RIG-I*-KO and a RIG-I overexpression B16-F10 cell line. The proliferation, cell cycle, apoptosis, migration and tumorigenesis activity in these cells were detected using CCK-8, BrdU incorporation assays, Annexin V/PI staining, Transwell assay and a xenograft tumor model

*in vivo*, respectively. The results indicated that RIG-I suppress the proliferation of but enhance the apoptosis of melanoma cells, both in the spontaneous state and upon poly I:C stimulation. Furthermore, target deletion of RIG-I results in faster growth rate of tumor xenografts, and Ki67 staining and TUNEL analysis also confirmed that RIG-I knockout promotes melanoma cell proliferation but inhibits melanoma cells apoptosis in vivo.

The MAPK signaling pathway has a central role in the regulation of cell cycle and apoptosis. Poly I:C has been proved to activate p38 MAPK through a membrane receptor TLR3 in several cell types. However, the potential role of p38MAPK in the cytosolic receptor mediated recognition of poly I:C remains to be addressed [28]. To elucidate the detailed molecular mechanism underlying the modulation of melanoma cell growth by RIG-I, we analyzed the expression and phosphorylation levels p38 MAPK. Western blot analysis revealed that RIG-I deficiency significantly suppressed the activation of p38 MAPK. We further investigated the expression and phosphorylation of two main MAP kinase kinases upstream of p38 MAPK: MKK3 and MKK4, and found their activities were inhibited by RIG-I knock out. These results were further confirmed in the RIG-I overexpression model. Given that p38 MAPK not only negatively regulates cell proliferation, but also exhibits proapoptotic function [29, 30], we postulated that p38 MAPK is responsible for the RIG-I-mediated change of cell growth in melanoma cells.

Taken together, the current study presented a novel role of RIG-I in the inhibition of cell proliferation and induction of apoptosis via modulating the phosphorylation of MKK3, MKK4 and p38 MAPK. Although more precise studies are needed to verify the molecular regulatory mechanism of RIG-I in the pathogenesis of melanoma, to the best of our knowledge, the current study is the first to demonstrate a possible role of RIG-I mediated activation of MKK/p38 signaling cascade in the proliferation and apoptosis of melanoma cells. Our findings might deepen the understandings of the antitumor function of RIG-I in melanoma, which could be useful to elucidate the pathogenesis and provide new therapeutic strategies of this malignant disease.

# Abbreviations

BrdU: Bromodeoxyuridine, CARDs: Caspase activation and recruitment domains, Cas9: CRISPR-associated protein 9, cDNA: Complementary DNA, CRISPR: Clustered regularly interspaced short palindromic repeats, DMEM: Dulbecco's Modified Eagle Medium, FBS: Fetal bovine serum, FITC: Fluorescein isothiocyanate, GAPDH: Glyceraldehyde 3-phosphate dehydrogenase, h: Hour, IKKα/IKKβ: IκB kinase α/ IκB kinaseβ, IRF3/IRF7: Interferon regulatory factor 3/ Interferon regulatory factor 7, KO: Knockout, MAPK: Mitogen-activated protein kinase, MAVS: Mitochondrial antiviral signaling protein, min: Minute, MKK3: Mitogen-activated protein kinase kinase 3, MKK4: Mitogen-activated protein kinase kinase 4, ml: Milliliter, MLK3: Mixed-lineage protein kinase 3, NC: Nitrocellulose, NF-κB: Nuclear factor kappa-B, PAM: Protospacer adjacent motif, PBS: Phosphate buffer solution, PBST: Phosphate Buffered Saline with Tween, PCR: Polymerase chain reaction, PFA: Paraformaldehyde, PI: Propidium iodide, Poly(I:C): Polyinosinic-polycytidylic acid, P-P38: Phospho-P38, RIG-I: Retinoic acid-inducible gene I, RIPA buffer:

Radioimmunoprecipitation assay buffer, RLR: RIG-I-like receptors, SDS: Sodium dodecyl sulfate, sgRNA: Small guide RNA, TBK1/IKK-i: TANK-binding kinase 1/ I-κB kinase, TLR3: Toll-like receptor 3.

# Declarations

### Ethics approval and consent to participate

Animal experimental manipulations were approved by the Animal Ethics Committee of Ruijin Hospital Affiliated to Shanghai Jiao Tong University School of Medicine.

### Consent for publication

Not applicable

### Availability of data and materials

The data used and/or analyzed during the current study are available from the corresponding author on reasonable request.

### Competing interests

The authors declared that they have no conflicts of interest.


### Funding

This work was supported by grants from the National Natural Science Foundation of China (81971462, 81671538 and 81901529) and Science and Technology Commission of Shanghai Municipality (201409001900, 19YF1430400).


### Authors' contributions

HZ and RG conceived and designed the study. RG, SL, QW, LZ, JM, YS, JW and CS performed the experiments. SL and LT generated cell lines. LL, ZW and HZ analyzed data. ZW and HZ wrote the paper. ZW and HZ were responsible for research supervision, coordination and strategy. RG and HZ confirm the authenticity of all the raw data. All authors have read and approved the final manuscript.


### Acknowledgements

Not applicable.



### Author details

[1]Research Center for Experimental Medicine, State Key Laboratory of Medical Genomics, Shanghai Ruijin Hospital, Shanghai Jiao Tong University School of Medicine, Shanghai 200025; [2]Shanghai Model

Organisms Center, Shanghai 201321; [3]Shanghai Institute of Immunology, Shanghai Jiao Tong University School of Medicine, Shanghai 200025.

# References

1. Schadendorf D, van Akkooi ACJ, Berking C, Griewank KG, Gutzmer R, Hauschild A, Stang A, Roesch A, Ugurel S. Melanoma The Lancet. 2018;392(10151):971–84. https://doi.org/10.1016/s0140-6736(18)31559-9.
2. Whiteman DC, Green AC, Olsen CM. The Growing Burden of Invasive Melanoma: Projections of Incidence Rates and Numbers of New Cases in Six Susceptible Populations through 2031. J Invest Dermatol. 2016;136(6):1161–71. https://doi.org/10.1016/j.jid.2016.01.035.
3. Leonardi GC, Falzone L, Salemi R, Zanghi A, Spandidos DA, McCubrey JA, Candido S, Libra M. Cutaneous melanoma: From pathogenesis to therapy (Review). Int J Oncol. 2018;52(4):1071–80. https://doi.org/10.3892/ijo.2018.4287.
4. Domingues B, Lopes JM, Soares P, Populo H. Melanoma treatment in review. Immunotargets Ther. 2018;7:35–49. https://doi.org/10.2147/ITT.S134842.
5. Read J, Wadt KA, Hayward NK. Melanoma genetics. J Med Genet. 2016;53(1):1–14. https://doi.org/10.1136/jmedgenet-2015-103150.
6. Paluncic J, Kovacevic Z, Jansson PJ, Kalinowski D, Merlot AM, Huang ML, Lok HC, Sahni S, Lane DJ, Richardson DR. Roads to melanoma: Key pathways and emerging players in melanoma progression and oncogenic signaling. Biochim Biophys Acta. 2016;1863(4):770–84. https://doi.org/10.1016/j.bbamcr.2016.01.025.
7. Pietrobono S, Anichini G, Sala C, Manetti F, Almada LL, Pepe S, Carr RM, Paradise BD, Sarkaria JN, Davila JI, et al. ST3GAL1 is a target of the SOX2-GLI1 transcriptional complex and promotes melanoma metastasis through AXL. Nat Commun. 2020;11(1):5865. https://doi.org/10.1038/s41467-020-19575-2.
8. Kadioglu O, Saeed MEM, Mahmoud N, Hussein Azawi SS, Rincic M, Liehr T, Efferth T. Identification of metastasis-related genes by genomic and transcriptomic studies in murine melanoma. Life Sci. 2021;267:118922. https://doi.org/10.1016/j.lfs.2020.118922.
9. Marie KL, Sassano A, Yang HH, Michalowski AM, Michael HT, Guo T, Tsai YC, Weissman AM, Lee MP, Jenkins LM, et al. Melanoblast transcriptome analysis reveals pathways promoting melanoma metastasis. Nat Commun. 2020;11(1):333. https://doi.org/10.1038/s41467-019-14085-2.
10. Chow KT, Gale M Jr, Loo YM. RIG-I and Other RNA Sensors in Antiviral Immunity. Annu Rev Immunol. 2018;36:667–94. https://doi.org/10.1146/annurev-immunol-042617-053309.
11. Yoneyama M, Kikuchi M, Natsukawa T, Shinobu N, Imaizumi T, Miyagishi M, Taira K, Akira S, Fujita T. The RNA helicase RIG-I has an essential function in double-stranded RNA-induced innate antiviral responses. Nat Immunol. 2004;5(7):730–7. https://doi.org/10.1038/ni1087.

12. Luo D, Ding SC, Vela A, Kohlway A, Lindenbach BD, Pyle AM. Structural insights into RNA recognition by RIG-I. Cell. 2011;147(2):409–22. https://doi.org/10.1016/j.cell.2011.09.023.
13. Seth RB, Sun L, Ea CK, Chen ZJ. Identification and characterization of MAVS, a mitochondrial antiviral signaling protein that activates NF-kappaB and IRF 3. Cell. 2005;122(5):669–82. https://doi.org/10.1016/j.cell.2005.08.012.
14. Kowalinski E, Lunardi T, McCarthy AA, Louber J, Brunel J, Grigorov B, Gerlier D, Cusack S. Structural basis for the activation of innate immune pattern-recognition receptor RIG-I by viral RNA. Cell. 2011;147(2):423–35. https://doi.org/10.1016/j.cell.2011.09.039.
15. Chen N, Xia P, Li S, Zhang T, Wang TT, Zhu J. RNA sensors of the innate immune system and their detection of pathogens. IUBMB Life. 2017;69(5):297–304. https://doi.org/10.1002/iub.1625.
16. Xu XX, Wan H, Nie L, Shao T, Xiang LX, Shao JZ. RIG-I: a multifunctional protein beyond a pattern recognition receptor. Protein Cell. 2018;9(3):246–53. https://doi.org/10.1007/s13238-017-0431-5.
17. Liu F, Wu S, Ren H, Gu J. Klotho suppresses RIG-I-mediated senescence-associated inflammation. Nat Cell Biol. 2011;13(3):254–62. https://doi.org/10.1038/ncb2167.
18. Zhu H, Xu WY, Hu Z, Zhang H, Shen Y, Lu S, Wei C, Wang ZG. RNA virus receptor Rig-I monitors gut microbiota and inhibits colitis-associated colorectal cancer. J Exp Clin Cancer Res. 2017;36(1):2. https://doi.org/10.1186/s13046-016-0471-3.
19. Wang Y, Zhang HX, Sun YP, Liu ZX, Liu XS, Wang L, Lu SY, Kong H, Liu QL, Li XH, et al. Rig-I-/- mice develop colitis associated with downregulation of G alpha i2. Cell Res. 2007;17(10):858–68. https://doi.org/10.1038/cr.2007.81.
20. Hou J, Zhou Y, Zheng Y, Fan J, Zhou W, Ng IO, Sun H, Qin L, Qiu S, Lee JM, et al. Hepatic RIG-I predicts survival and interferon-alpha therapeutic response in hepatocellular carcinoma. Cancer Cell. 2014;25(1):49–63. https://doi.org/10.1016/j.ccr.2013.11.011.
21. Ma H, Jin S, Yang W, Zhou G, Zhao M, Fang S, Zhang Z, Hu J. Interferon-alpha enhances the antitumour activity of EGFR-targeted therapies by upregulating RIG-I in head and neck squamous cell carcinoma. Br J Cancer. 2018;118(4):509–21. https://doi.org/10.1038/bjc.2017.442.
22. Li Y, Song Y, Li P, Li M, Wang H, Xu T, Yu X, Yu Y, Tai Y, Chen P, et al. Downregulation of RIG-I mediated by ITGB3/c-SRC/STAT3 signaling confers resistance to interferon-alpha-induced apoptosis in tumor-repopulating cells of melanoma. J Immunother Cancer. 2020;8(1). https://doi.org/10.1136/jitc-2019-000111.
23. Besch R, Poeck H, Hohenauer T, Senft D, Hacker G, Berking C, Hornung V, Endres S, Ruzicka T, Rothenfusser S, et al. Proapoptotic signaling induced by RIG-I and MDA-5 results in type I interferon-independent apoptosis in human melanoma cells. J Clin Invest. 2009;119(8):2399–411. https://doi.org/10.1172/JCI37155.
24. Zhang HX, Liu ZX, Sun YP, Zhu J, Lu SY, Liu XS, Huang QH, Xie YY, Zhu HB, Dang SY, et al. Rig-I regulates NF-kappaB activity through binding to Nf-kappab1 3'-UTR mRNA. Proc Natl Acad Sci U S A. 2013;110(16):6459–64. https://doi.org/10.1073/pnas.1304432110.

25. Duewell P, Steger A, Lohr H, Bourhis H, Hoelz H, Kirchleitner SV, Stieg MR, Grassmann S, Kobold S, Siveke JT, et al. RIG-I-like helicases induce immunogenic cell death of pancreatic cancer cells and sensitize tumors toward killing by CD8(+) T cells. Cell Death Differ. 2014;21(12):1825–37. https://doi.org/10.1038/cdd.2014.96.
26. Sato J, Azuma K, Kinowaki K, Ikeda K, Ogura T, Takazawa Y, Kawabata H, Kitagawa M, Inoue S. Combined Use of Immunoreactivities of RIG-I with Efp/TRIM25 for Predicting Prognosis of Patients With Estrogen Receptor-positive Breast Cancer. Clin Breast Cancer. 2020. https://doi.org/10.1016/j.clbc.2020.12.001.
27. Chen L, Feng J, Wu S, Xu B, Zhou Y, Wu C, Jiang J. Decreased RIG-I expression is associated with poor prognosis and promotes cell invasion in human gastric cancer. Cancer Cell Int. 2018;18:144. https://doi.org/10.1186/s12935-018-0639-3.
28. Paone A, Starace D, Galli R, Padula F, De Cesaris P, Filippini A, Ziparo E, Riccioli A. Toll-like receptor 3 triggers apoptosis of human prostate cancer cells through a PKC-alpha-dependent mechanism. Carcinogenesis. 2008;29(7):1334–42. https://doi.org/10.1093/carcin/bgn149.
29. Bulavin D, Fornace AJ. p38 MAP Kinase's Emerging Role as a Tumor Suppressor. Adv Cancer Res. 2004;92:95–118. https://doi.org/10.1016/S0065-230X(04)92005-2.
30. Moriwaki K, Asahi M. Augmented. TME O-GlcNAcylation Promotes Tumor Proliferation through the Inhibition of p38 MAPK. Mol Cancer Res. 2017;15(9):1287–98. https://doi.org/10.1158/1541-7786.MCR-16-0499.

# Figures

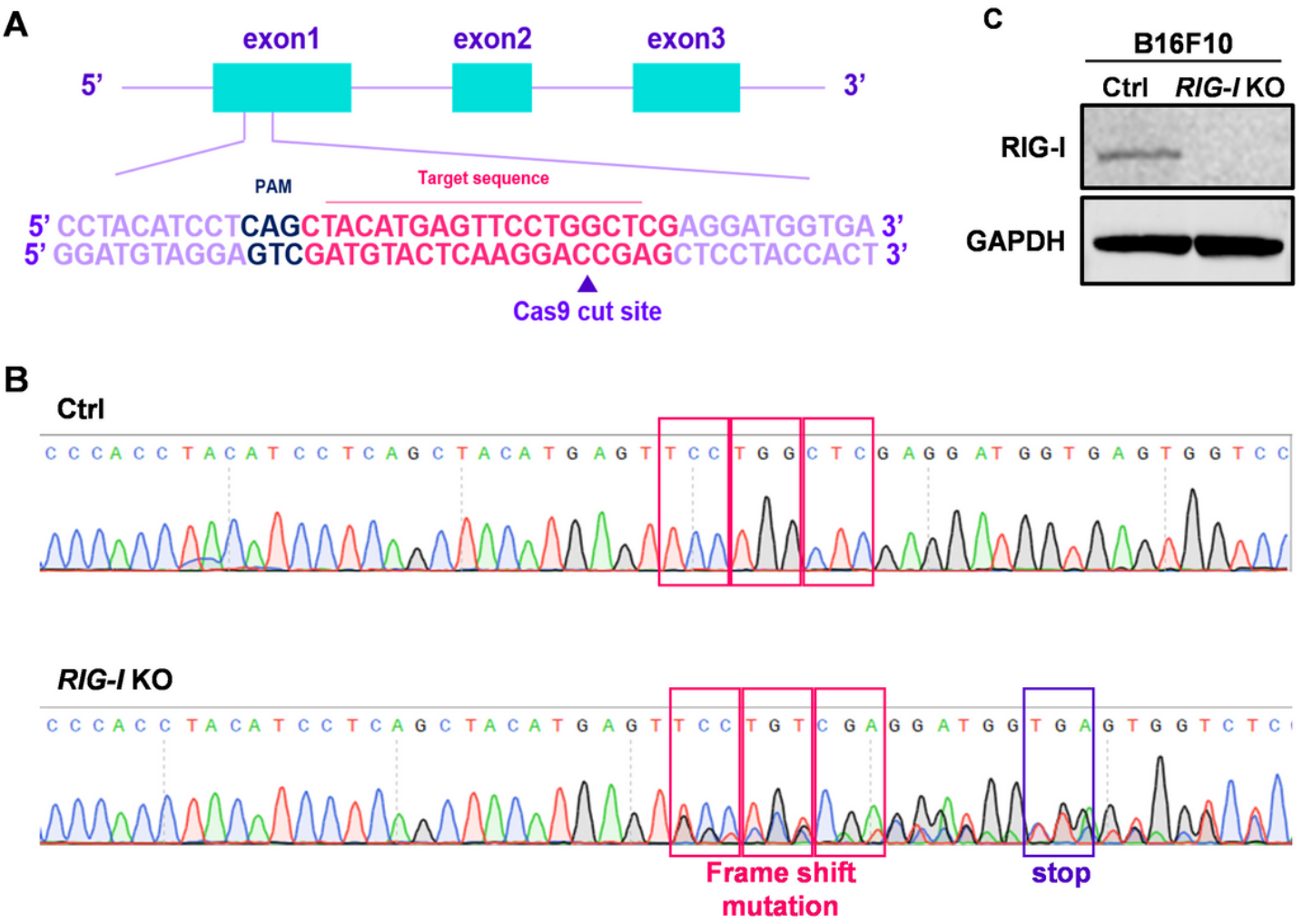


## Figure 1

Generation and validation of RIG-I knockout in B16-F10 cells. (A) Schematic of the gRNA target site of RIG-I knockout cells. PAM sequence is marked in dark blue. The arrow indicates the cleavage site by Cas9. (B) Two bases of nucleic acid were deleted and resulting in frameshift mutation and the translation termination by a stop codon after the mutant site in RIG-I KO B16-F10 cells by DNA sequencing. (C) The control and RIG-I KO cells were analyzed by Western blotting with anti-RIG-I antibody. Anti-GAPDH antibody was used as a loading control.

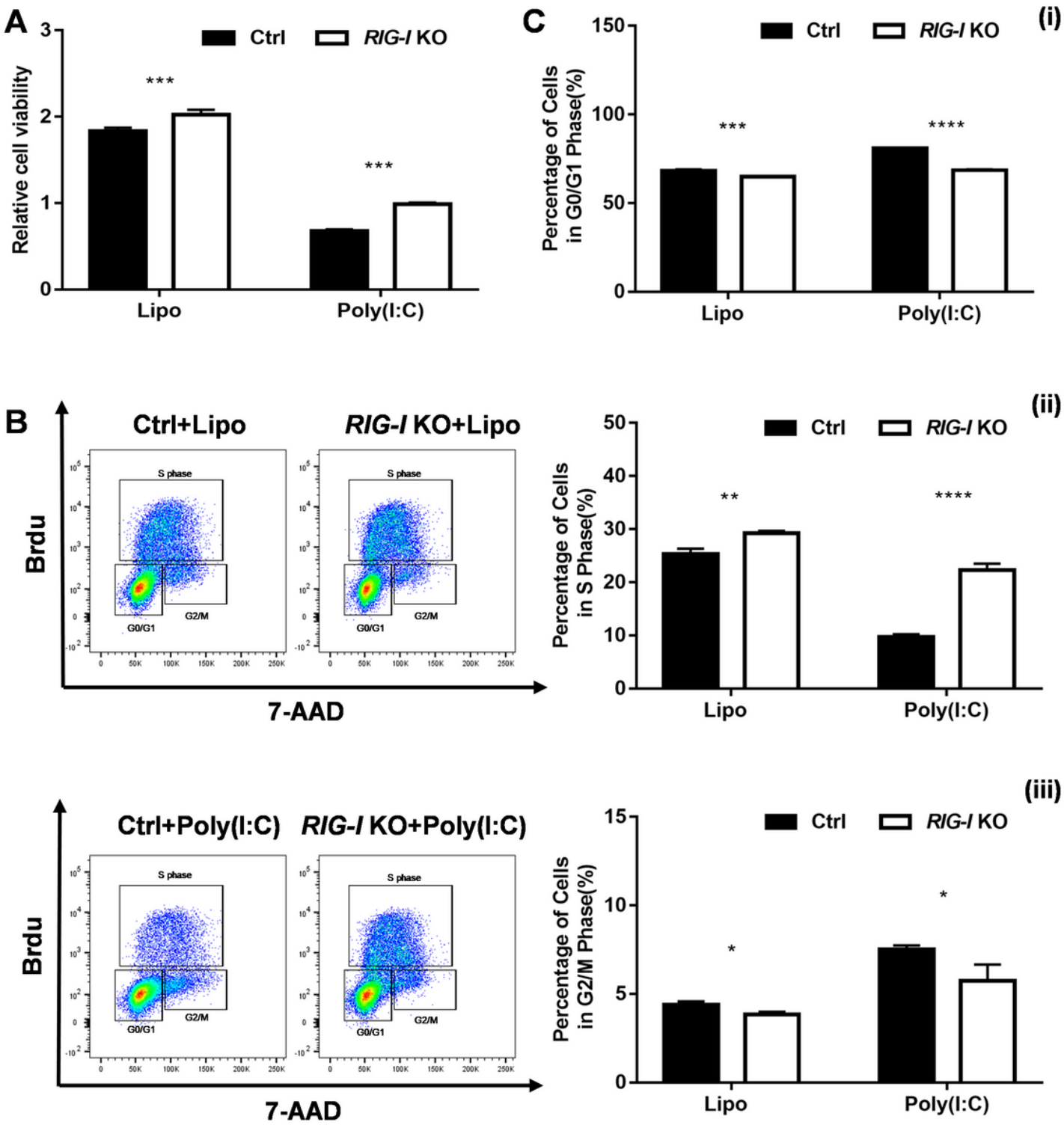


## Figure 2

Target deletion of RIG-I promotes the proliferation of B16-F10 cells. (A) CCK-8 assay was performed to evaluate the cell viability in Ctrl and RIG-I KO B16-F10 cells with or without Poly(I:C) (10μg/ml) for 24h. The cell viability ratio was calculated by the following formula: cell viability (%) =OD (24h)/OD (average of 0h) ×100%. n= 4 , *** p< 0.001. (B) BrdU incorporation and FACS analyses for control and RIG-I-KO B16-F10 cells treated with with Poly(I:C) (10μg/ml) or Lipofectamine 3000. (C) Percentages of different stages

of the cell cycle were calculated. n=3 in each group. (i) Percentage of cells in G0/G1 phase. (ii) Percentage of cells in S phase. (iii) Percentage of cells in G2/M phase. *P<0.05, **P<0.01, *** P<0.001, **** P<0.0001.

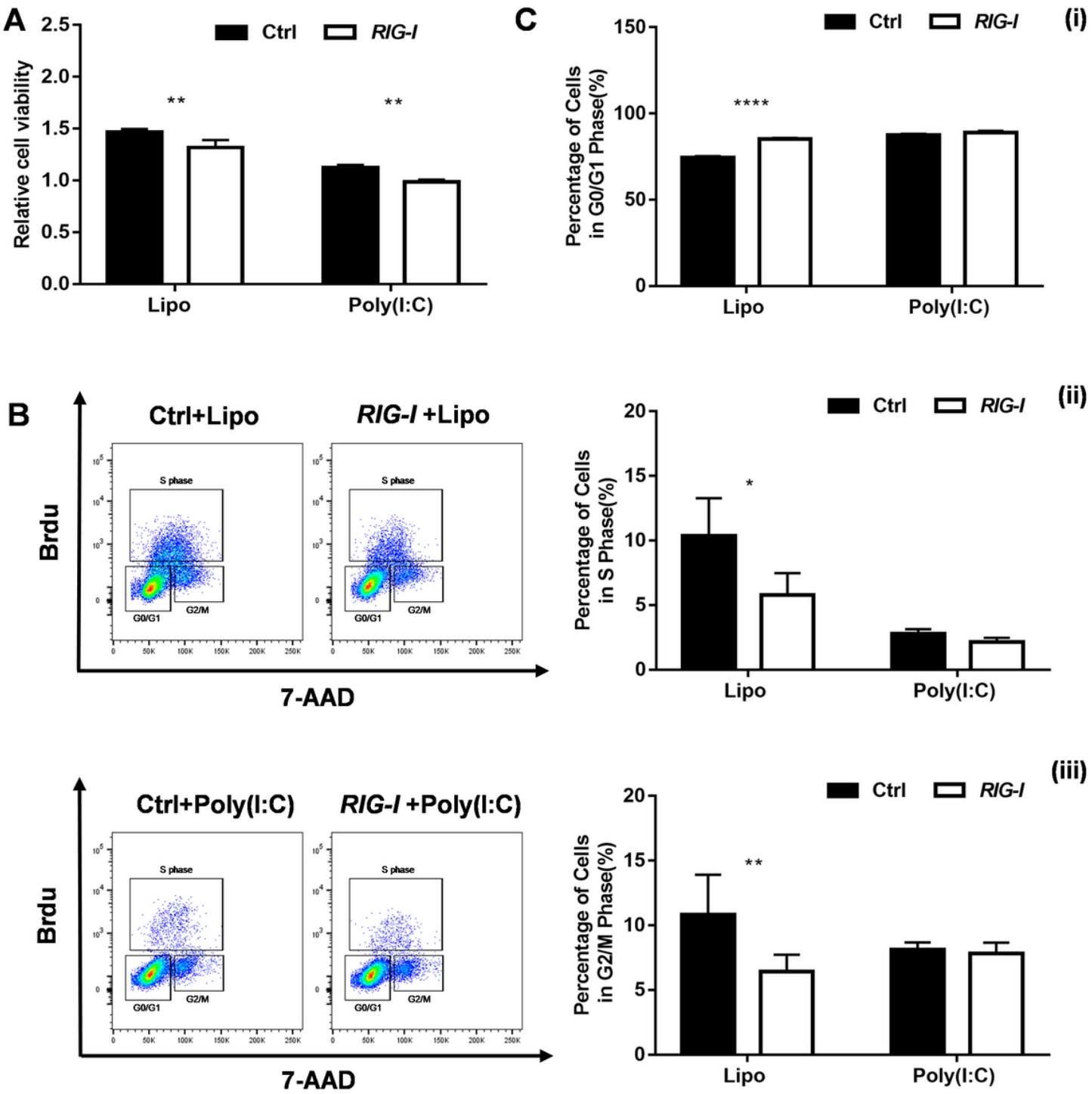


## Figure 3

Ectopic overexpression of RIG-I inhibits the proliferation of B16-F10 cells. (A) CCK-8 assay was performed to evaluate the cell viability in Ctrl and RIG-I overexpression B16-F10 cells with or without Poly(I:C) (10μg/ml) for 24h. n= 4 , *** p< 0.001. (B) BrdU incorporation and FACS analyses for control and RIG-I-KO

B16-F10 cells treated with Poly(I:C) (10μg/ml) or Lipofectamine 3000. (C) Percentages of different stages of the cell cycle were calculated. n=3 in each group. (i) Percentage of cells in G0/G1 phase. (ii) Percentage of cells in S phase. (iii) Percentage of cells in G2/M phase. *P<0.05, **P<0.01, **** P<0.0001.

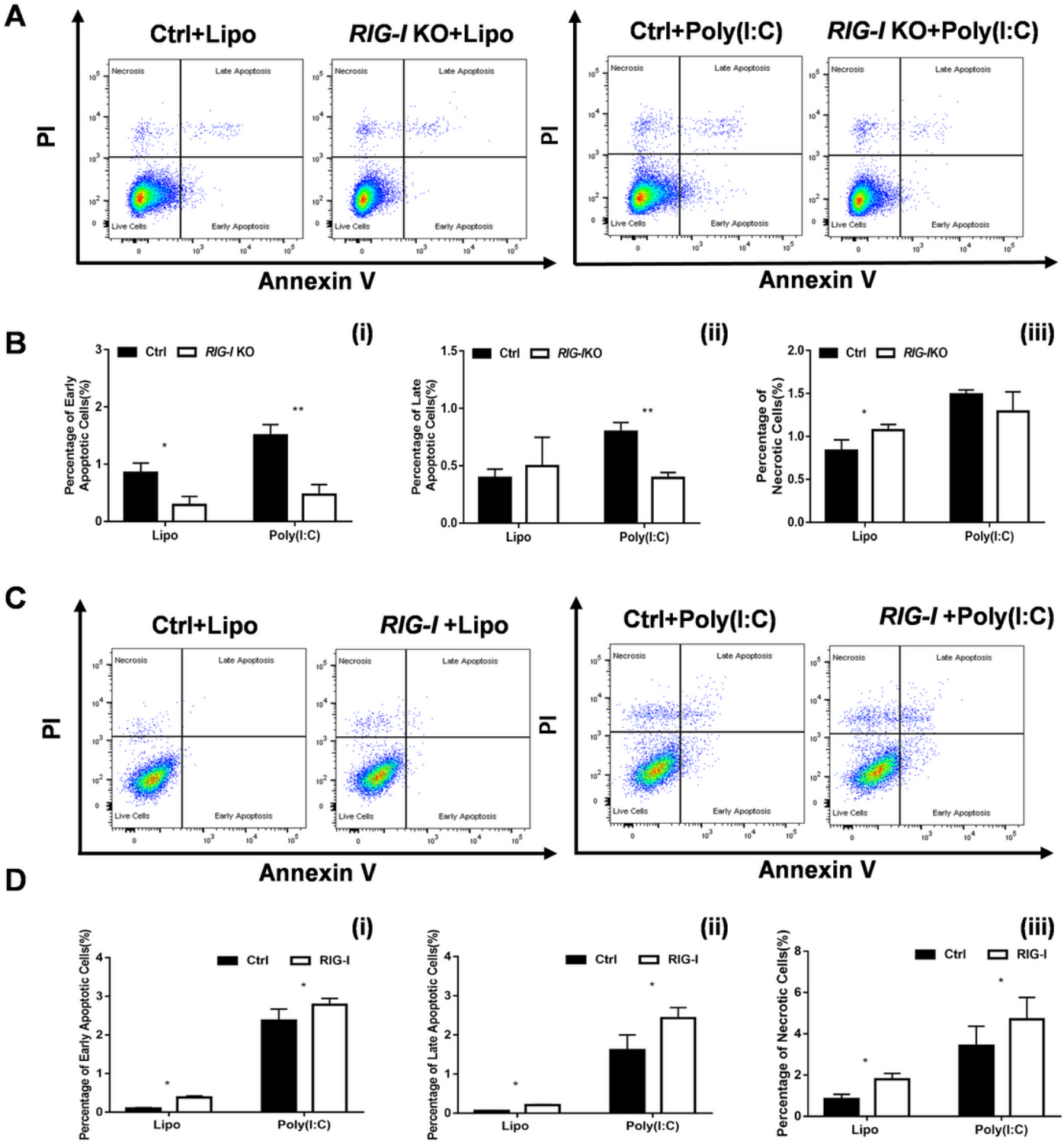


## Figure 4

Effects of RIG-I KO and RIG-I overexpression on the apoptosis of B16-F10 cells. (A) Flow cytometry analysis of apoptosis in Ctrl and RIG-I KO B16-F10 cells treated with Poly(I:C) (10μg/ml) or Lipofectamine 3000. (B) Percentages of different stages of apoptotic cells were calculated. (i) Early apoptosis: Annexin

V+/PI-, (ii) Late apoptosis: Annexin V+/PI+, (iii) Necrosis: Annexin V-/PI+. *P<0.05, **P<0.01. (C, D) Flow cytometry analysis of apoptosis of Ctrl and RIG-I overexpression B16-F10. *P<0.05.

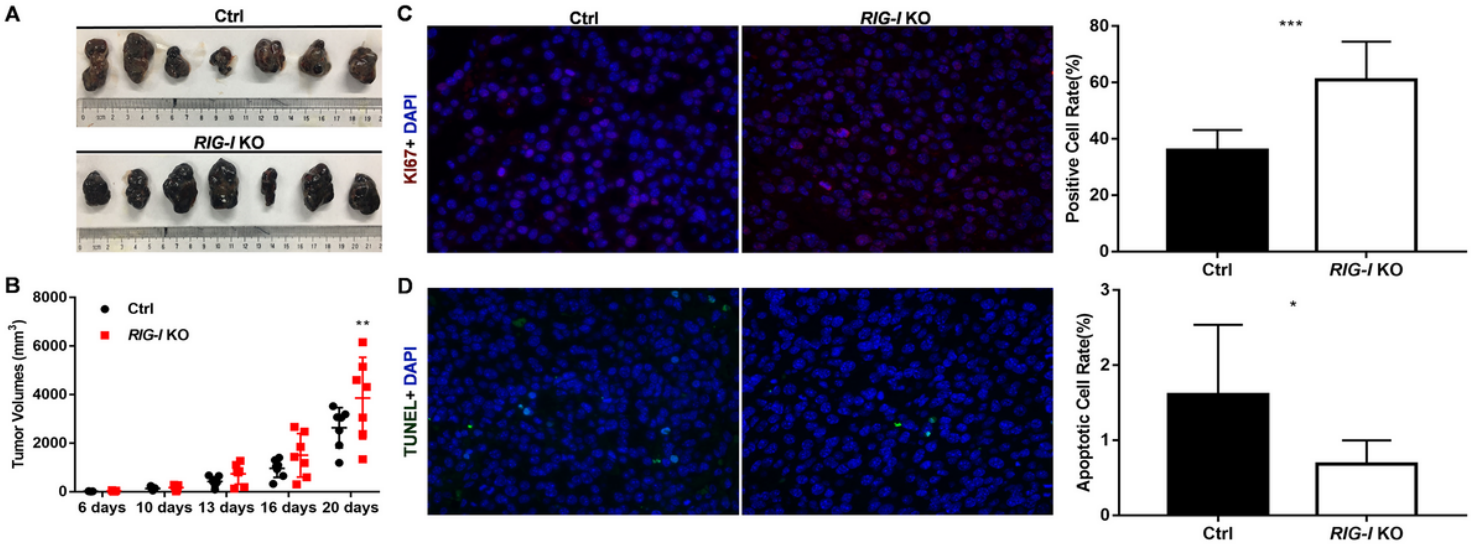


## Figure 5

Knockout of RIG-I enhances the growth of B16-F10 cell xenografts in nude mouse model. (A) Images of the tumors isolated from the nude mice model derived from RIG-I KO and control B16-F10 melanoma cells (n=7). (B) Tumor volume was calculated by the following formula: Tumor Volume (mm3) = (length x width2)/2. **P<0.01. (C) Cell proliferation was assessed by Ki67 staining. KI67-positive cell proportions were quantified by Image J and calculated as follows: Positive Cell Rate (%) =KI67+ cells (depicted as red fluorescence)/total number of cells per photo (represented by blue nuclei stain, DAPI). (D) TUNEL staining was utilized to measure melanoma cell apoptosis in tumors. TUNEL-positive cell proportions were quantified by ImageJ and calculated as follows: Apoptotic Cell Rate (%) =TUNEL-positive cells (depicted as green fluorescence)/total number of cells per photo (represented by blue nuclei stain, DAPI). *P<0.05, ***P<0.001.

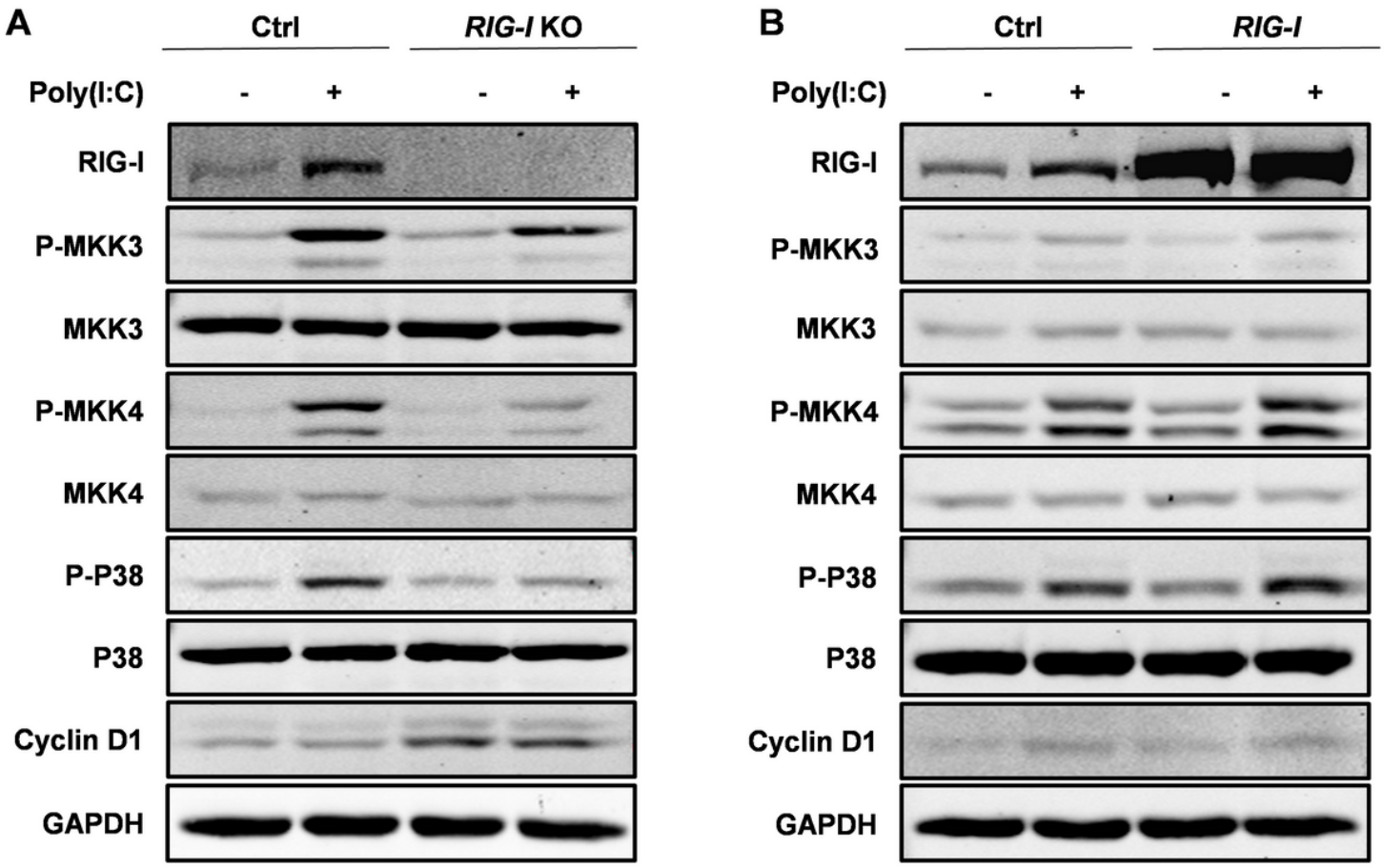


**Figure 6**

RIG-I exerts anti-tumor effects through MKK/p38 MAPK signaling pathway in B16-F10 cells. (A) Ctrl and RIG-I KO B16-F10 melanoma cells were transfected with Poly(I:C) (10μg/ml) or Lipofectamine 3000 for 24h, respectively. The total and phosphorylation protein levels of MKK3, MKK4, P38, Cyclin D1 were examined by western blot assay. GAPDH served as loading control. (B) Ctrl and RIG-I overexpression B16-F10 melanoma cells were transfected with Poly(I:C) (10μg/ml) or Lipofectamine 3000 for 24h, respectively. The western blot assay was conducted as panel A.

## Supplementary Files

This is a list of supplementary files associated with this preprint. Click to download.

- AuthorChecklist.pdf
- Supplementaryfigures.pdf